DEVELOPMENT AND VALIDATION OF A COARSE-GRAINED MODEL FOR THE BIOCOMPATIBLE POLYMER POLYCAPROLACTONE

By

ABHINAV SANKARA RAMAN

A thesis submitted to the

Graduate School – New Brunswick

Rutgers, The State University of New Jersey

In partial fulfillment of the requirement

For the degree of

Master of Science

Graduate Program in Chemical and Biochemical Engineering

Written under the direction of

Dr. Yee C. Chiew

and approved by

_____

_____

_____

_____

New Brunswick, New Jersey

May, 2016

ABSTRACT OF THE THESIS

DEVELOPMENT AND VALIDATION OF A COARSE-GRAINED MODEL FOR THE BIOCOMPATIBLE POLYMER POLYCAPROLACTONE

by ABHINAV SANKARA RAMAN

Thesis Director:

Dr. Yee C. Chiew

Polycaprolactone (PCL), is a biocompatible polyester with many applications towards the betterment of human health. The advent of superior computational power and novel simulation techniques such as coarse-grained molecular dynamics simulations, enable the in-silico study of processes involving nano-polymeric materials over large spatio-temporal scales. In this study, a coarse-grained model for PCL was developed within the framework of the MARTINI coarse-grained (CG) force field. The non-bonded interactions were based on the existing MARTINI bead types, while the bonded interactions were mapped from the OPLS-UA/AA rendition of PCL. The developed model accurately reproduced the structural and dynamic properties of the PCL homopolymer, also showing reasonably good temperature and solvent transferability. We also studied the self-assembly of MePEG-b-PCL linear diblock copolymers using an existing MARTINI model for MePEG (Methoxy Polyethylene glycol), by analyzing the critical micelle concentration, as well as the shape, size and morphology of the nano-polymeric micelles. We obtained excellent agreement of the critical micelle concentration, while the size was under-predicted compared to experimental data.

Acknowledgements

First and foremost, I would like to thank my advisor Dr. Yee Chiew, for taking me under his tutelage. It was both a privilege and honor to work under someone I have always considered as one of my heroes and inspiration, with respect to my scientific pursuits. Science aside, I would also like to thank him for imbibing in me his impeccable research ethics and character, which I'm certain will stay with me for the rest of my life. I would also like to thank Dr. Aleksey Vishnyakov for his valuable input and discussions with respect to this project.

I would like to thank my family for their support over all these years. This would not have been possible without their help. I would like to thank all my friends, especially Subhodh and Srinivas, for all their help over these three years. I would like to thank J.R.R Tolkien for writing the Lord of the Rings, whose heroes have inspired and lifted my spirit on several occasions. Finally, I would like to thank God, for at the end of the day, none of this would have happened if not for his unrequited love.

Table of Contents

List of Tables

List of Figures

Chapter 1

Introduction

Poly-ε-caprolactone (PCL), an FDA approved biodegradable hydrophobic polyester, has been used widely in the biomaterials arena, showing a resurgence in the last decade. PCL, has known applications in the medical devices field ranging from sutures and wound dressings to dentistry. However, it is the birth and boom of tissue engineering that has re-vitalized the importance of PCL as a biomaterial. Due to its far superior rheological properties, cost-efficient production and longer degradation time, it is now widely applied as long term implants and scaffolds with huge potentials for bettering human health. In addition to these, PCL has always been used in nanoparticle based drug delivery systems, making it one of the few biomaterials with versatile applications[1].

Its use in nanoparticle based drug delivery devices is one of potential importance in treatment of diseases and ailments such as cancer, owing to novel properties such as targeted delivery and controlled release of drugs[2, 3]. In a large number of cases, PCL is functionalized with ligands or other functional groups, and the resulting copolymers are used for drug delivery. Specifically, amphiphilic copolymers formed by functionalizing PCL with a hydrophilic functional group, and the block copolymer micelles that they form, have shown to evade the reticuloendothelial system, thereby providing a much improved circulation time for the nano-carriers[4, 5]. Of the many amphiphilic systems studied with PCL, the polyethylene glycol block polycaprolactone (PEG-b-PCL) is one that has been widely applied[6, 7].

Over the last decade, the advent of superior computational power, and the use of mesoscale simulation techniques such as coarse-grained molecular dynamics simulations, have aided in a large number of computational studies on the behavior of polymeric molecules, especially amphiphiles, such as diblock star copolymers[8], peptides[9], and triblock copolymers[10] to name a few. A recent review paper by Thota and Jiang[11], on computational studies involving amphiphilic materials used specifically for drug delivery applications, goes to show the importance of developing robust and accurate models for such systems. Specifically with respect to PCL and the diblock PEG-PCL copolymer, it is worth noting the CG model of Loverde et al.[12], which reproduces the phase diagram of the PEG-PCL system. Further, the authors also studied the effect of the shape of the nanoparticle on drug delivery, by analyzing the loading of the popular anti-cancer drug Taxol into self-assembled nanoparticles. While there are several other standalone CG models for a large number of polymers, including other amphiphiles, transferability of CG models is problematic and requires a systematic development across different classes of compounds.

In this study, we have developed a model for PCL within the framework of the popular MARTINI coarse-grained (CG) force field[13, 14]. The MARTINI force field, originally developed for lipids, is a systematically parametrized CG biomolecular force field suitable for molecular dynamics simulations of a large number of biomolecules. While molecular models for a large number of molecules such as lipids, proteins and sugars have been developed for use with the MARTINI force field, only a few polymers have been covered. The prominent examples include polyethylene oxide (PEO) and polyethylene glycol (PEG) by Lee et al.[15], Polystyrene by Rossi et al.[16], PAMAM by Lee and Larson[17] and more

recently for Pluronics by Nawaz and Carbone[18]. This serves as further motivation for the development of models for biocompatible polymers such as PCL, aiding in the extension of the force field for simulating more molecules.

The objective of this study is to develop CG force field parameters for PCL that can be applied to polymer solutions and amphiphilic macromolecular systems within the MARTINI framework. The proposed coarse-grained model was then validated against conformational and structural properties based on atomistic models or experimental data. We found that the proposed PCL model proves to be a robust CG model for this important biopolymer.

This thesis is organized as follows. Chapter 2 provides a description of the CG force field for PCL and the parametrization of the intramolecular interactions of the PCL homopolymer and the MePEG-b-PCL linear copolymer. Chapter 3 discusses the computational details of the simulations performed as part of this study. This is followed by the validation of the homopolymer model against structural and dynamic properties, and the copolymer model against the self-assembly of amphiphiles, in Chapter 4. Owing to the rising popularity and computational advantages of implicit-solvent simulations, the transferability of the developed model for PCL to an implicit solvent version of the MARTINI force field is discussed in Chapter 5. The thesis closes with the conclusions in Chapter 6.

Chapter 2

Forcefield Development

In line with the common MARTINI coarse-graining procedure, each particle in the PCL model represents four heavy atoms and associated hydrogens. Therefore, the PCL repeat unit is modelled by two interaction centers. The ester part is modeled as a non-polar acceptor bead ('Na' MARTINI bead type), while the alkyl $(CH_2)_4$ part is modeled as an apolar 'C1' MARTINI bead type. The model for MePEG was taken from Lee et al.[15] The mapping of both the molecules is schematically shown in Fig.1. The non-bonded interactions in the CG model (LJ 12-6 potential) are based on the interaction parameter matrix developed in the improved and extended MARTINI version described in Marrink et al., [13] with modifications to the PEO-PEO and PEO-water interactions suggested in refs[19, 20] . The beads were connected by harmonic bonds and angles, obtained by fitting the molecular conformations of CG models of select oligomers, to those obtained in atomistic MD simulations performed with the OPLS-UA[21] and OPLS-AA[22] forcefields. The oligomers were divided into fragments according to the coarse-graining scheme shown in Fig. 1, and the distributions of distances and angles between the beads of the CG model were matched to the distributions of distances and angles between the centers of mass of the corresponding fragments.

The bond stretching and the angle bending potentials were optimized to reproduce the distributions obtained from the all-atom simulations, as shown in Figure 2. The complete set of bonded interaction parameters and the functions used to model them are given in Table 1. Inclusion of the dihedral term could have made the agreement between the CG

and atomistic models even better, but we have opted to avoid 4-body terms due to a higher computational cost, taking into account the spatial and temporal scales involved in the self-assembly of triblock copolymers. It was found that the proposed model is able to represent the properties of PCL and MePEG-*b*- PCL very well (see Chapter 4).

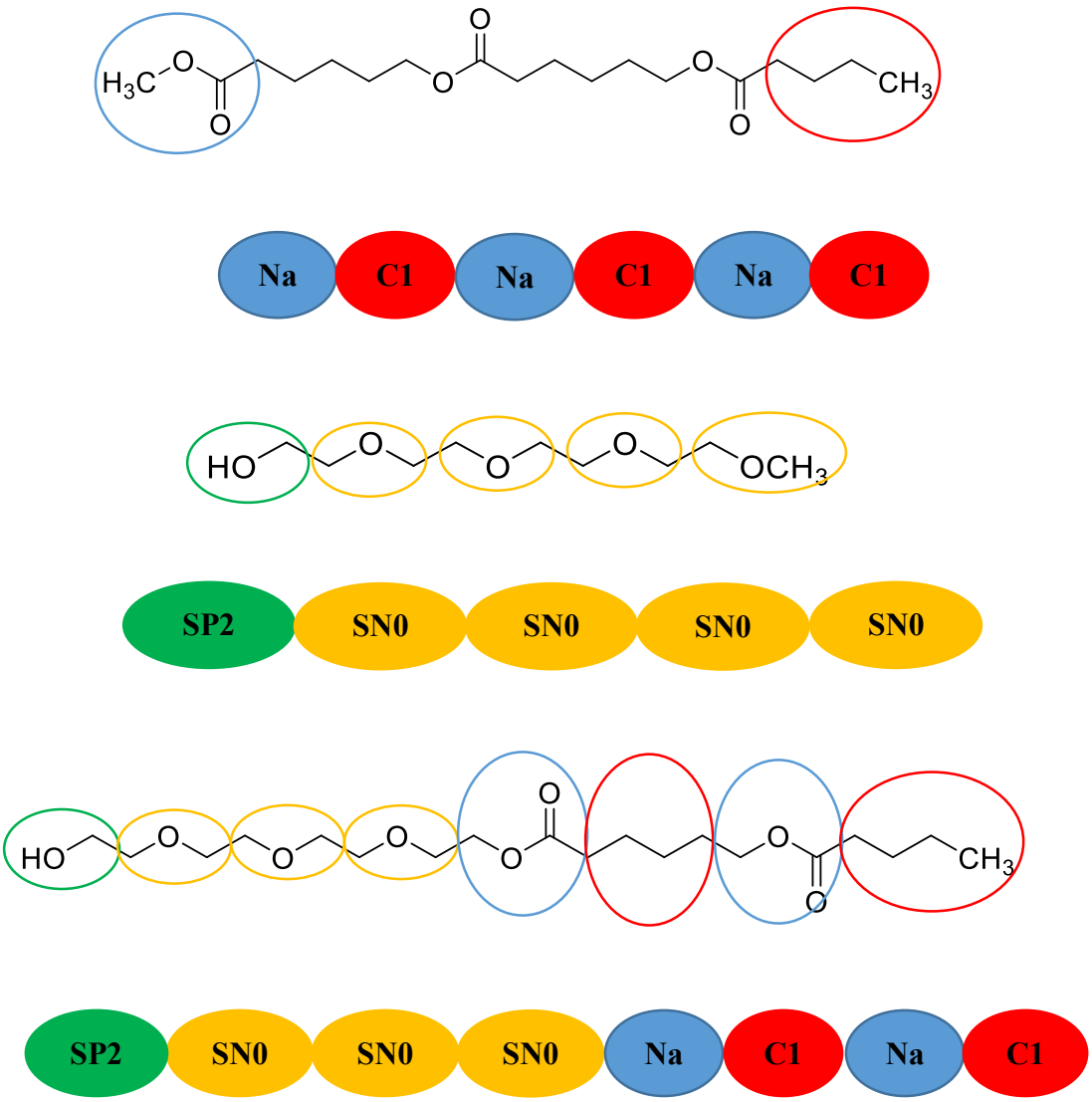

Fig.1 Mapping scheme and the corresponding MARTINI-CG rendition of PCL (top) MePEG (middle) and MePEG-b-PCL (bottom).

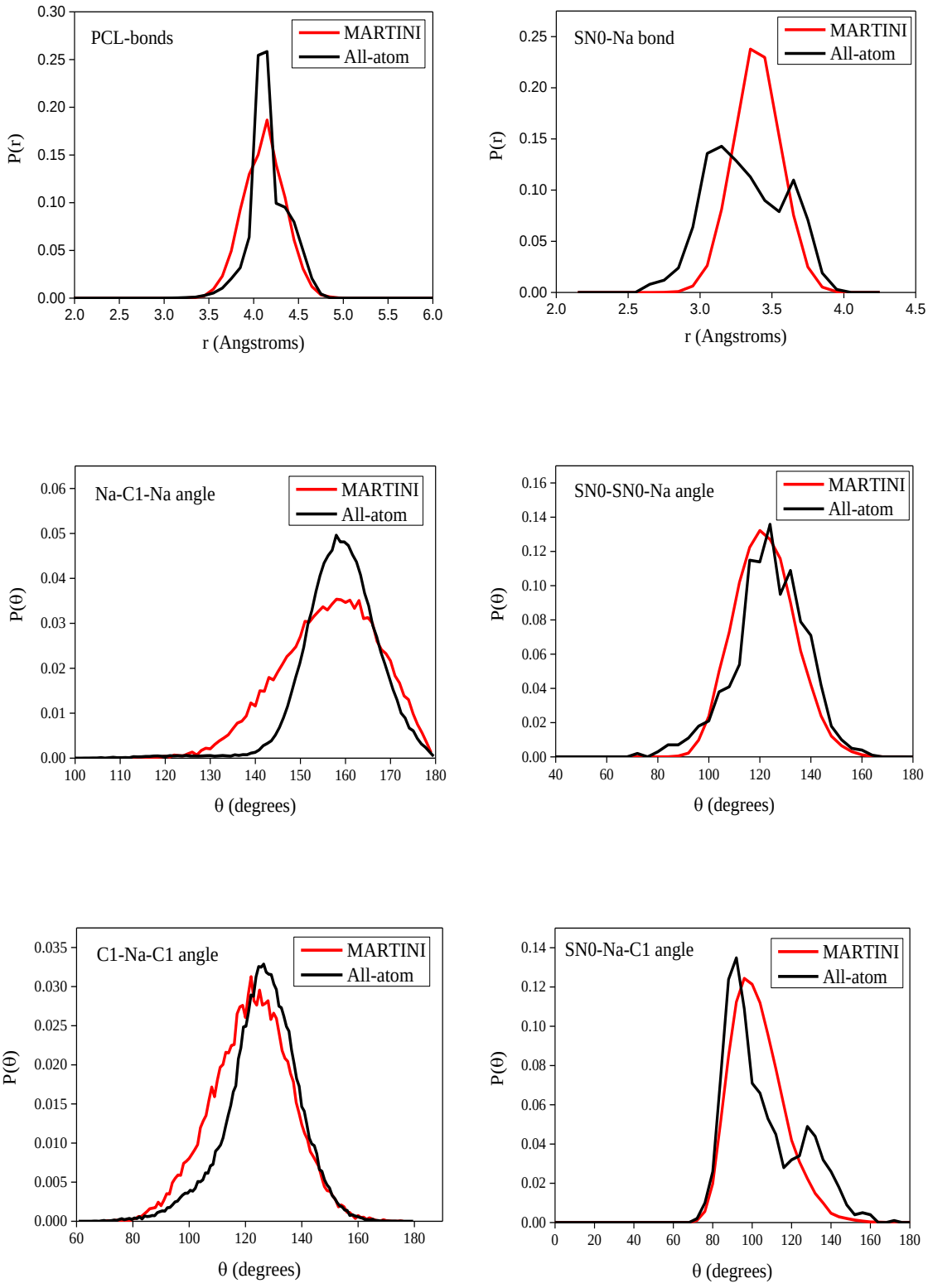

Fig.2 PCL bond and angle distribution (left: top to bottom), MePEG-PCL interconnecting beads bond and angle distribution (right: top to bottom).

Table 1. Parameters of the bonded interactions in the CG model

		Bond		Angle	
		r_o (nm)	**K_b (kJ/mol nm^2)**	**θ_o (degrees)**	**K_θ (kJ/mol)**
PCL:	Na-C1	0.415	5000		
	Na-C1-Na			170	40
	C1-Na-C1			129	40
MePEG-PCL:	SN0-Na	0.340	10000		
	SN0-SN0-Na			122	50
	SN0-Na-C1*			102	40

The function used to model bond stretching: $V_b(r) = {}^1\!/_2\, K_b(r - r_o)^2$; angle bending: $V_{angle}(\theta) = {}^1\!/_2\, K_\theta(\theta - \theta_o)^2$, * $V_{angle}(\theta) = {}^1\!/_2\, K_\theta(cos\theta - cos\theta_o)^2$

Chapter 3

Computational Details

The parametrization of the intramolecular interactions in the PCL homopolymer were obtained by mapping from an OPLS-UA rendition of PCL, while those for the co-polymer were obtained from an OPLS-AA rendition in SPC (simple point charge)[23] water. In both cases, atomistic simulations of short chains in solution were performed to obtain the distribution of the bonds and angles. Corresponding MARTINI coarse-grained simulations of short chains in MARTINI water were performed to obtain the optimized bonded parameters of the CG force field. The developed model for the homopolymer was then validated by comparing structural and dynamic properties of different chain lengths in solution against atomistic simulations using the OPLS-AA force field and SPC water. The starting configuration of the polymer in both the cases was obtained by briefly simulating the chain in vacuum, allowing it to coil up. Suitable box sizes were then chosen based on the approximate radius of gyration of the homopolymers. All the atomistic simulations for the homopolymer were performed for 50-100ns, while the corresponding CG simulations were performed for 1μs. Self-assembly of the MePEG-b-PCL copolymers were then studied via coarse-grained simulations, performed over 1.5-2μs, with a starting configuration obtained by placing monomers at random locations in a cubic box typically 20nm x 20nm x 20nm in dimensions. The specific details of the atomistic and CG simulations are discussed below.

3.1 Atomistic Simulations

As discussed above, the atomistic simulations were done using the OPLS-AA force field, performed using the Gromacs[24, 25] molecular simulation package. A 2fs time step was employed, with the bonds constrained using the LINCS[26] algorithm. A cut-off of 1.0nm was used for both the van der Waals and Coulombic interactions, with analytical tail corrections for the dispersion interactions to account for the finite cut-off. Long range electrostatics were dealt with using the Particle Mesh Ewald (PME)[27] method. All the simulations were performed in the isothermal-isobaric ensemble (NPT), with the temperature controlled using a velocity-rescale[28] thermostat and a coupling time of 0.1ps. For equilibration purposes, the pressure was controlled using a Berendsen[29] barostat with a coupling time of 1.0ps, and compressibility of $4.5*10^{-5}$ bar^{-1}, while the production runs used the Parrinello-Rahman[30] barostat with a coupling time of 2.0ps. The reference pressure was set to 1.0 bar.

3.2 Coarse-grained Simulations

The MARTINI coarse-grained simulations were all performed using the Gromacs molecular simulation package, with a time step of 20fs for the homopolymers and 10fs for the copolymers. A smaller integration time step was found to be more stable with the copolymers owing to the torsion and bending potentials employed in the MARTINI model for PEG and PEO[15]. It should however be noted that larger time steps can be employed with the newly improved potentials suggested by Bulacu et al.[31]. The shift function starting at 0.9nm with a cut-off of 1.2nm was used for the dispersion

interactions. All the simulations were performed in an isothermal-isobaric (NPT) ensemble, with the temperature controlled using a velocity-rescale[28] thermostat and a coupling time of 1.0ps. Similar to the atomistic simulations, the Berendsen[29] barostat with a coupling time of 4.0ps was used for equilibration purposes, and the Parrinello-Rahman[30] barostat with a coupling time of 6.0ps was used in the production runs. A compressibility of $5*10^{-6}$ bar^{-1} was used, with the reference pressure set to 1.0 bar.

3.3 Implicit Solvent Simulations

The implicit solvent simulations were all performed with the "Dry MARTINI" force field developed by Arnarez et al.[32], using the second-order stochastic dynamics (SD) integrator in the Gromacs molecular simulation package. The simulations were all performed in the NVT ensemble, with a time step of 40fs for integrating the equations of motion. The temperature was set to 300K, with an inverse friction coefficient of 4.0ps used to set the friction in the Langevin equation. For testing the transferability of the CG potential (bond stretching, angle bending), short simulations of 200-500ns were done on both dilute melts of short PCL segments as well as isolated long chains, while simulations of 1μs were performed for analyzing the conformation of select PCL homopolymers. The dispersion interactions were modelled as described above for the "wet MARTINI" case. In all the simulations performed in this study, periodic boundary conditions were applied on all three directions.

Chapter 4

Results and Discussion

4.1 PCL homopolymer: Structural and conformational properties

The validation of the developed CG model for PCL begins with the study on the conformation of PCL homopolymers of different chain lengths in water at 300K. The conformation of the CG homopolymers in MARTINI water was compared against atomistic simulations using an OPLS-AA representation of PCL in SPC water. In cases where the atomistic simulations were not performed by us, results from a recent work on atomistic simulations of PCL in water and acetone by Di Pasquale et al.[33] have been taken. Table 2 shows the time averaged end to end distance and Table 3, the time averaged radius of gyration of the homopolymers investigated.

Table 2. Time averaged end to end distance of PCL homopolymers in water (nm) (mean $\pm$ SD) at 300K

N	MARTINI-CG	OPLS-AA (Di Pasquale et al.[33])	OPLS-AA This work
10	1.36 ± 0.56	1.34 ± 0.48	-
20	1.41 ± 0.54	1.47 ± 0.5	-
30	1.51 ± 0.60	1.69 ± 0.6	1.5 ± 0.55
50	1.77 ± 0.61	-	1.94 ± 0.46
75	1.97 ± 0.75	-	2.24 ± 0.48

Table 3. Time averaged radius of gyration of PCL homopolymers in water (nm) (mean $\pm$ SD) at 300K

N	MARTINI-CG	OPLS-AA (Di Pasquale et al.[33]) (Mean Radius of gyration)	OPLS-AA This work
10	0.76 ± 0.13	0.64	-
20	0.83 ± 0.04	0.77	-
30	0.92 ± 0.03	0.88	0.89 ± 0.03
50	1.08 ± 0.02	-	1.03 ± 0.02
75	1.23 ± 0.02	-	1.16 ± 0.01

Fig.3 plots the radius of gyration R_g against the number of repeat units, with the resulting plot fitted to the scaling relation:

$$R_g = aN^{\nu} \qquad [1]$$

where, R_g is the radius of gyration, N is the number of monomeric repeat units, a is a fitting constant and ν is the Flory exponent[34]. From the fit, we obtained a Flory exponent of 0.297 (~ 0.30), which was found to be in excellent agreement with the all-atom simulation results of Di Pasquale et al[33] ($\nu \sim 0.3$), and the theoretical value of 1/3 for a polymer chain in a poor solvent. This clearly shows that water is a poor solvent for the hydrophobic PCL. Table 4 shows a comparison of the principal moments of the gyration tensor for select PCL chains between the CG and all-atom models. Clearly, the good agreement of the principal moments indicate that the CG and all-atom models predict a similar shape for the PCL chains in water.

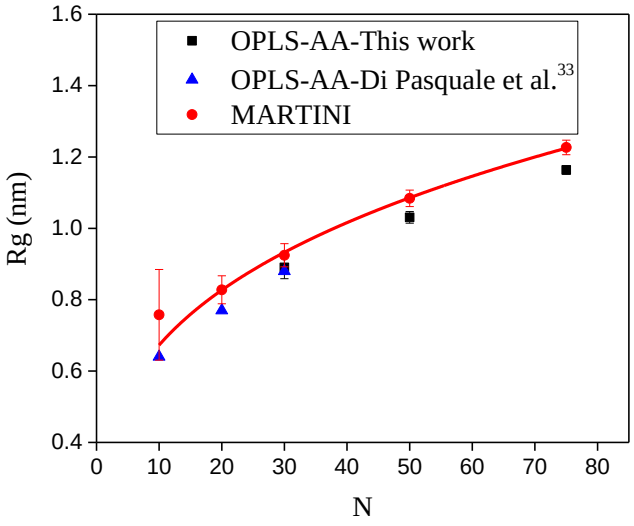

Fig.3 Radius of gyration versus number of monomeric repeat units for PCL homopolymer in water. The red solid line is an exponential fit of the MARTINI data points using Eq.1.

Table 4. Time averaged principle moments of the gyration tensor of PCL homopolymers in water (nm) (mean ± SD) at 300K

N	MARTINI-CG			OPLS-AA-This work		
	λ_1	λ_2	λ_3	λ_1	λ_2	λ_3
30	0.64 ± 0.06	0.51 ± 0.03	0.41 ± 0.03	0.63 ± 0.06	0.49 ± 0.03	0.40 ± 0.03
50	0.74 ± 0.05	0.61 ± 0.03	0.50 ± 0.03	0.69 ± 0.04	0.58 ± 0.03	0.50 ± 0.02
75	0.82 ± 0.05	0.70 ± 0.03	0.59 ± 0.03	0.76 ± 0.03	0.65 ± 0.02	0.58 ± 0.02

4.2 PCL homopolymer: Temperature transferability of the model

The MARTINI-CG force field, as with most biomolecular force fields is typically parametrized at ambient conditions (300K and ambient pressure). Since applications may

entail the simulation of systems at different thermodynamic states, the transferability of the developed model becomes vital. Further, it has been shown by Carbone et al.[35] that a generic transferability of the force field usually does not work, and that it has to be verified on a molecule to molecule basis. Therefore, we performed simulations at three temperatures (283.15, 323.15 and 343.15K) for select PCL homopolymers in water (ambient 1bar pressure). As above, the MARTINI-CG simulations were compared against atomistic simulations performed using the OPLS-AA force field and the SPC water model. The resulting time averaged radius of gyration is given in Table 5. It can clearly be seen that both the MARTINI-CG and atomistic simulations predict a small increase in the radius of gyration with increasing temperature, owing to the well-known fact of weakened hydrogen bonds in water at higher temperatures. From the table, it is also clear that water still remains a poor solvent for the hydrophobic PCL, with the MARTINI-CG model also capturing this, and therefore showing good temperature transferability.

Table 5. Time averaged radius of gyration of PCL homopolymers in water (nm) over a range of temperatures (K) (mean $\pm$ SD)

Temp. (K)	**MARTINI-CG**			**OPLS-AA-This work**		
	PCL-30	**PCL-50**	**PCL-75**	**PCL-30**	**PCL-50**	**PCL-75**
283.15	0.92 $\pm$ 0.03	1.07 $\pm$ 0.02	1.21 $\pm$ 0.02	0.88 $\pm$ 0.02	1.02 $\pm$ 0.02	1.16 $\pm$ 0.01
323.15	0.94 $\pm$ 0.04	1.09 $\pm$ 0.03	1.23 $\pm$ 0.02	0.89 $\pm$ 0.02	1.05 $\pm$ 0.02	1.18 $\pm$ 0.02
343.15	0.96 $\pm$ 0.04	1.11 $\pm$ 0.03	1.25 $\pm$ 0.02	0.90 $\pm$ 0.03	1.05 $\pm$ 0.02	1.19 $\pm$ 0.02

4.3 PCL homopolymer: Dynamics of PCL in solution

The diffusion constant *D* of a polymeric micelle is related to its hydrodynamic radius R_h via the Stokes-Einstein relation[15] given below:

$$R_h = \frac{k_B T}{6\pi\eta D} \quad [2]$$

where, R_h is the hydrodynamic radius, T is the absolute temperature, k_B is the Boltzmann constant, D is the diffusion constant and η is the viscosity of the medium. The above equation indicates that the diffusion constant is inversely related to the viscosity of the medium, suggesting that it may not provide a good comparison of the dynamics, since the viscosities can be very different between the atomistic and coarse-grained solvents. A better and more suitable approach to compare dynamics, is to use the hydrodynamic radius, which is a measure of both the conformation and the interaction between the polymer and the solvent, and is therefore expected to be similar between different simulation methods (all atom and CG) and experiment.

Here, we compared the hydrodynamic radius of select PCL homopolymers in water, between the MARTINI-CG model in regular MARTINI water and the OPLS-AA rendition in SPC water at 300K. The viscosity of the MARTINI water model was taken from Fuhrmans et al.[36] and for the SPC water model from Hess[37]. The diffusion constant was corrected for finite size effects based on the formula derived by Yeh and Hummer[38] given below:

$$D = D_{PBC} + \frac{k_B T \xi}{6\pi\eta L} \quad [3]$$

where, D_{PBC} is the diffusion constant obtained with periodic boundary conditions, ξ = 2.837297 and L is the length of the cubic simulation cell. In our simulations, D_{PBC} was obtained from a linear fit of the mean squared displacement (MSD) of the homopolymer, and then corrected for finite size effects as described above. Table 6 shows the comparison of the hydrodynamic radius between the MARTINI-CG and all-atom model for select PCL homopolymers in water. It can be seen that while PCL-30 and PCL-50 show accurate hydrodynamic radii compared to the atomistic results, PCL-75 is an anomaly in that it shows a smaller hydrodynamic radii than PCL-50. Similar anomalies have also been reported in Lee et al.[15] for PEO homopolymers, and is largely attributed to statistical uncertainties.

Table 6. Hydrodynamic radius of PCL homopolymers in water (nm) (mean $\pm$ SD)

N	MARTINI-CG	OPLS-AA-This work
30	0.64 ± 0.24	0.53 ± 0.19
50	1.19 ± 0.16	1.32 ± 0.12
75	0.92 ± 0.05	1.54 ± 0.25

4.4 PCL homopolymer: Solvent transferability of the model

In a recent paper, Di Pasquale et al[33] investigated the conformational and structural behavior of PCL in a binary water-acetone mixture via atomistic simulations. The authors highlighted the process called solvent displacement which principally involves the dissolution of the polymer in a good solvent followed by rapid mixing with an anti-solvent. This technique seems to be a popular route for the production of nanoparticles based on PCL.[39, 40] Therefore, we investigated the solvent transferability of the CG model

by studying the structural conformation of PCL homopolymers in mixtures of acetone and water of varying compositions. We initially performed simulations with the regular MARTINI water model, but found that the mixture effects and the solvent structuring around the PCL homopolymer were poorly represented (not shown here). Therefore, the solvent transferability was tested using the more accurate polarizable MARTINI water model[41], despite a higher computational cost. When using the polarizable MARTINI water model, Coulombic interactions were modeled using a shifted Coulombic potential with a 1.2nm cut-off in an implicit dielectric medium with $\varepsilon = 2.5$.

Table 7 shows the time averaged end to end distance and Table 8, the time averaged radius of gyration of select PCL homopolymers at four different solvent compositions. PCL is known to interact favorably with acetone (where PCL is expected to accept a coil-like conformation) and unfavorably with water. It should be noted that the solvent composition around the polymers is inhomogeneous and anisotropic, since the polymer attracts the favorable solvent. Even at small bulk acetone fractions, it has a significant presence around the PCL molecules, as reported by Di Pasquale et al[33]. They observed an abrupt globule-to-coil transition of PCL chains approximately corresponding to the equimolar solution of acetone and water (x_A=0.5) rather than a smooth transformation from globules to coils as x_A increased. Tables 7 and 8 show that the MARTINI-CG model of PCL is able to accurately capture the PCL conformations in both globule (observed at x_A =0) and coil (observed at x_A =1 and x_A=0.75) states, but generally predicts smoother globule-to-coil transformations. Only for the shortest PCL homopolymer investigated in this study (PCL-10), a good agreement between the atomistic and CG representations was

obtained. Both PCL-20 and PCL-30 undergo a gradual transformation from coil to globule conformation as the water content increases.

This observation may reflect general features of CG models (for example, gradual expansion-contraction transformations rather than distinct transitions were recently obtained in DPD simulations of polymer brushes in mixed solvents[42]). However, the atomistic models may also be at fault here, as the common atomistic force fields (including the OPLS-AA model) and other newer modifications are as yet unable to reproduce the complete miscibility of acetone in water over the entire composition range. This inaccuracy of the solvent model can artificially sharpen the coil-globule transition. Overall, the MARTINI-CG model shows good solvent transferability, but care must be taken when modelling the behavior in mixtures.

Table 7. Time averaged end to end distance of PCL homopolymers (nm) in acetone-water mixture (mean ± SD)

x_A	**MARTINI-CG (Polarizable MARTINI water)**			**OPLS-AA-Di Pasquale et al.** [33]		
	PCL-10	**PCL-20**	**PCL-30**	**PCL-10**	**PCL-20**	**PCL-30**
1	3.93 ± 1.29	4.94 ± 2.06	6.13 ± 2.66	3.21 ± 1.13	4.72 ± 2.7	6.22 ± 2.0
0.75	3.35 ± 1.35	3.60 ± 1.65	5.36 ± 2.82	3.21 ± 1.10	4.15 ± 1.4	5.50 ± 1.9
0.5	2.98 ± 1.37	2.38 ± 1.11	2.24 ± 0.92	3.01 ± 1.10	4.07 ± 1.7	4.82 ± 1.8
0	1.25 ± 0.53	1.37 ± 0.54	1.48 ± 0.53	1.34 ± 0.48	1.47 ± 0.5	1.69 ± 0.6

Table 8. Time averaged radius of gyration of PCL homopolymers (nm) in acetone-water mixture (mean ± SD)

x_A	MARTINI-CG (Polarizable MARTINI water)			OPLS-AA-Di Pasquale et al. [33] (Mean radius of gyration)		
	PCL-10	**PCL-20**	**PCL-30**	**PCL-10**	**PCL-20**	**PCL-30**
1	1.50 ± 0.25	2.10 ± 0.46	2.44 ± 0.64	1.25	1.85	2.42
0.75	1.38 ± 0.26	1.65 ± 0.45	2.22 ± 0.77	1.23	1.73	2.17
0.5	1.28 ± 0.30	1.24 ± 0.21	1.24 ± 0.18	1.19	1.66	2.06
0	0.72 ± 0.12	0.82 ± 0.03	0.92 ± 0.03	0.64	0.77	0.88

4.5 Copolymer model: Self-assembly of amphiphilic diblock copolymers

PCL based nanoparticles, especially block copolymer micelles formed from PEG-PCL copolymers have found numerous applications in the field of drug-delivery. Therefore, to validate the copolymer model developed for the MePEG-b-PCL linear diblock copolymer described in Chapter 2 above, we studied their self-assembly to analyze the morphology, shape and size of the micelles formed, and compare them with experimental data. Particularly we studied the $MePEG_{17}$-b-PCL_3 and $MePEG_{17}$-b-PCL_2 systems due to the availability of experimental hydrodynamic radius and critical micelle concentration (CMC) as reported by Letchford et al.[43]. Since the CMC for the $MePEG_{17}$-b-PCL_3 system is too low to be simulated at reasonable simulation cell sizes, we do not consider it here. The $MePEG_{17}$-b-PCL_2 system has a reasonably large CMC which serves as a useful quantity for validating the model.

4.5.1 Morphology, size and shape of the self-assembled micelles

We analyzed the self-assembly of randomly placed monomers in MARTINI water at 300K as well as the physiological temperature of 310K. Fig.4 depicts a series of snapshots at different times through the course of the simulation at 300K, clearly describing the self-assembly process of the $MePEG_{17}$-b-PCL_3 system. The initial configuration was obtained by placing 240 monomers at random positions throughout the simulation cell.

We find that within 200ns, most of the monomers formed small aggregates, which then combined to form large spherical micelles on a 1μs timescale. Beyond this, and until the end of the simulation, we did not find any coalescence of the formed micelles, nor their dissociation. This is also quantitatively described in Fig.5 showing the time evolution of the number of clusters present in the system. In our analysis, we consider two molecules to be part of a cluster if the distance between the hydrophobic PCL beads is less than or equal to 0.55nm. It should also be noted that the value of this cut-off was not arbitrarily chosen, and is based on the position of the first peak of the radial distribution function between PCL beads.

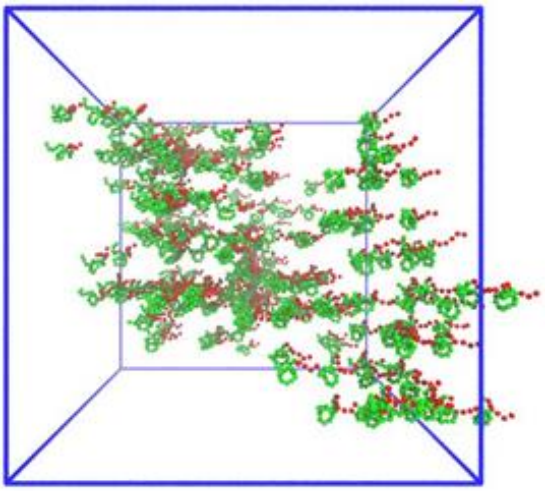

t=0ns

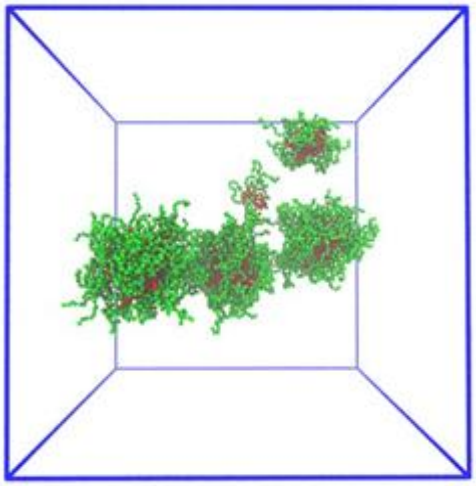

t=200ns

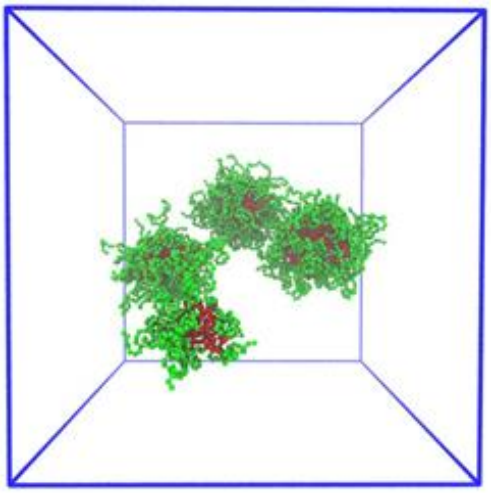

t=500ns

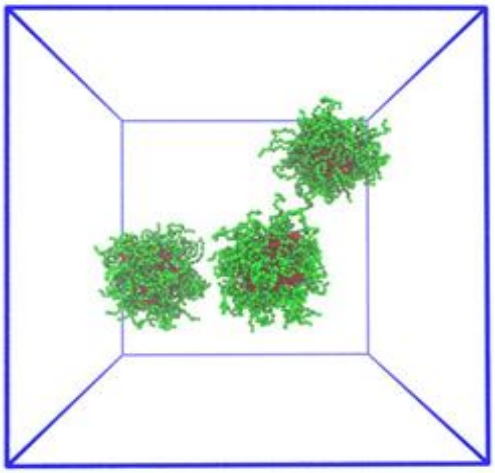

t=1000ns

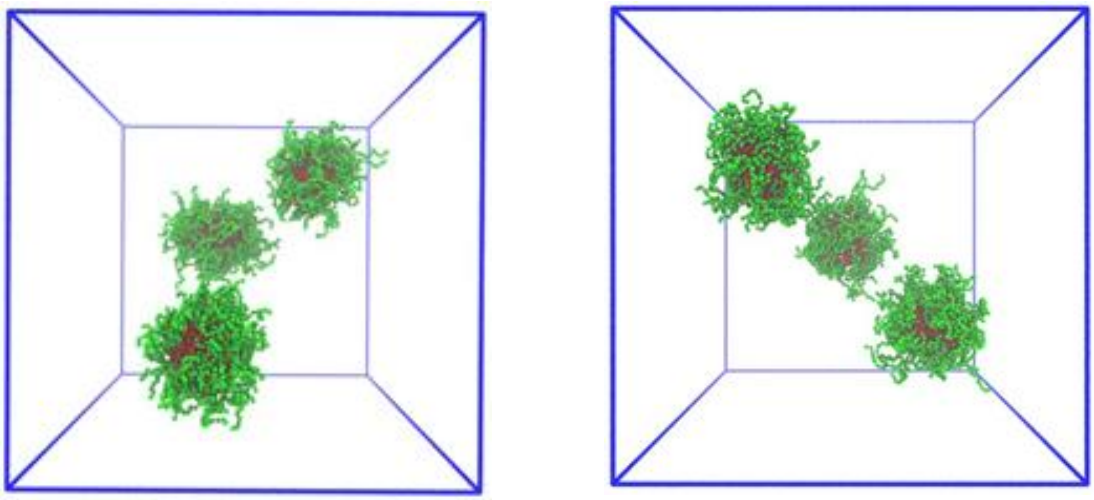

Fig.4 Snapshots of the self-assembly of the $MePEG_{17}$-b-PCL_3 system at 300K, through the course of the simulation. (Color codes: MePEG-Green, PCL-Red) (Solvent has been removed for clarity).

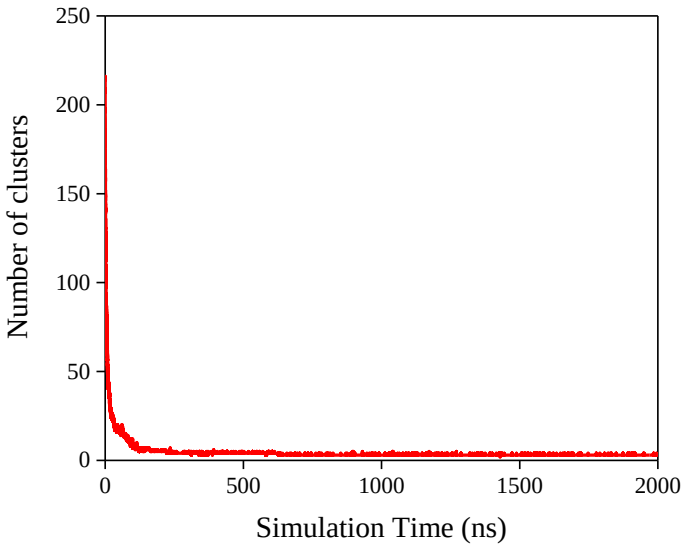

Fig.5 Time evolution of the number of clusters for the $MePEG_{17}$-b-PCL_3 system at 300K.

From Fig.4, it is also clear that the micelles possess a core-shell morphology with PCL forming the dense hydrophobic core and the hydrophilic MePEG forming the shell. The morphology of the largest aggregate is shown in Fig.6, which describes the local density variation of PCL and MePEG beads with respect to the center of mass (COM) of the micelle. The local density profile of water with respect to the COM of the micelle is given in the inset, clearly showing the exclusion of water from the hydrophobic PCL core.

Table 9 gives the mean cluster size, radius of gyration and asphericity of the micelles obtained from the $MePEG_{17}$-b-PCL_3 system at 300K. It is fairly clear from Table 9 that the micelles are pretty much spherical, with asphericity values less than 0.005.

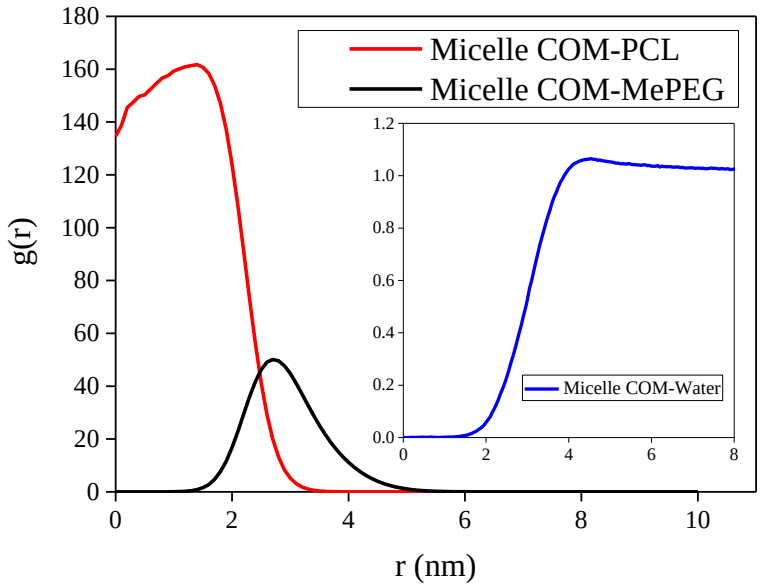

Fig.6 Morphology of the biggest cluster at 300K. The inset shows the local solvent (water) structure.

Table 9. Mean cluster size (number of molecules), radius of gyration (nm) and asphericity of the clusters ($MePEG_{17}$-b-PCL_3) at 300K (mean ± SD)

Mean cluster size	Radius of gyration	Asphericity
86	2.90 ± 0.03	0.0032 ± 0.0020
82	2.87 ± 0.03	0.0034 ± 0.0024
72	2.76 ± 0.03	0.0030 ± 0.0021

As discussed above, we also studied the self-assembly of the $MePEG_{17}$-b-PCL_3 and the $MePEG_{17}$-b-PCL_2 systems at 310K (not shown here). Over the same simulation time, we observed a similar evolution of the system as seen above at 300K. Micelles of similar shape and morphology were obtained, albeit with a different aggregation number, as seen in Tables 10 and 11.

Table 10. Mean cluster size (number of molecules), radius of gyration (nm) and asphericity of the clusters ($MePEG_{17}$-b-PCL_3) at 310K (mean ± SD)

Mean cluster size	Radius of gyration	Asphericity
112	3.17 ± 0.03	0.0052 ± 0.0034
65	2.68 ± 0.03	0.0027 ± 0.0017
63	2.67 ± 0.03	0.0034 ± 0.0021

Table 11. Mean cluster size (number of molecules), radius of gyration (nm) and asphericity of the clusters ($MePEG_{17}$-b-PCL_2) at 310K (mean ± SD)

Mean cluster size	Radius of gyration (nm)	Asphericity
81	2.96 ± 0.12	0.0121 ± 0.0074
79	2.87 ± 0.05	0.0078 ± 0.0049
73	2.84 ± 0.10	0.0086 ± 0.0054

4.5.2 Critical micelle concentration (CMC) and hydrodynamic radius

The hydrodynamic radius and the CMC serve as useful quantities for further validation of the developed model, due to the fact that they can be measured and quantified experimentally. The computation of the hydrodynamic radius follows the same procedure as outlined for the PCL homopolymers. Further, it should also be noted that since the change in viscosity of MARTINI water is minimal for a 10K change in temperature, we used the same viscosity reported above at ambient temperature, for the 310K case as well. Table 12 compares the hydrodynamic diameter of the biggest micelles obtained with the $MePEG_{17}$-b-PCL_3 and $MePEG_{17}$-b-PCL_2 systems at 310K, against experimentally measured values at the same temperature. It can be seen that the hydrodynamic diameter is under-predicted compared to the experimental data in both the cases. A similar behavior was also seen in a recent paper by Thota et al.[9] on self-assembled micelles formed from amphiphilic peptides modeled using the MARTINI-CG force field. As observed by Thota et al.[9], we feel that the finite simulation time and system size may be the cause for this discrepancy.

Table 12. Hydrodynamic diameter of the largest clusters (nm) at 310K (mean $\pm$ SD)

Mean cluster size (Simulation)	**Hydrodynamic diameter (Simulation)**	**Hydrodynamic diameter (Experimental- Letchford et al.[43])**
	$MePEG_{17}$-b-PCL_3	
112	9.09 ± 1.37	13.5 ± 0.3
	$MePEG_{17}$-b-PCL_2	
81	8.21 ± 0.08	11.1 ± 1.2

We also determined the CMC of the $MePEG_{17}$-b-PCL_2 system. Through the course of the simulation, we found that initially formed small aggregates later combined to larger micelles existing in dynamic equilibrium with monomers in solution. Fig.7 shows the time evolution of the number of free monomers and the aggregation number of the clusters formed. It can be seen that over the last 500ns of simulation time, the cluster size and the number of free monomers in solution remain roughly constant.

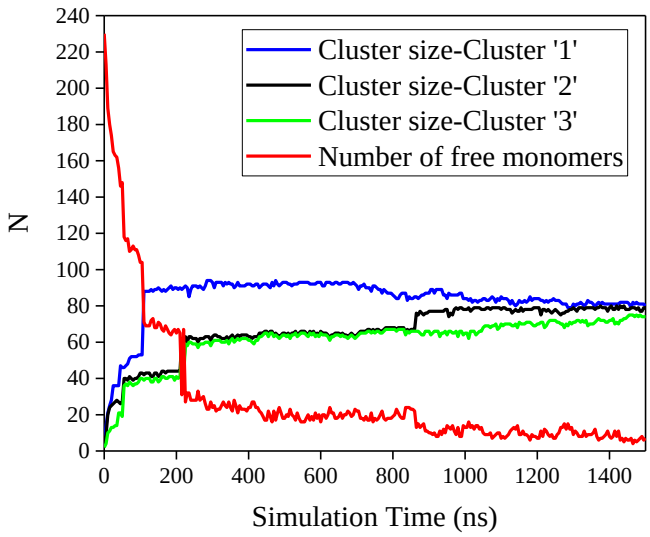

Fig.7 Time evolution of the number of free monomers and aggregation number of the clusters for the $MePEG_{17}$-b-PCL_2 system at 310K.

We obtained three clusters with the aggregation numbers of 81±1, 79±1 and 73±2 molecules, existing in dynamic equilibrium with 7±2 free monomers in solution (Total of 240 copolymer molecules in the simulation cell). Since we obtained only large micelles or free monomers, the use of counting rules to categorize smaller clusters as belonging to micelles or free monomers was obviated. The actual number of free monomers in solution

was taken as the CMC and converted to mmol/L. The computed CMC is compared with that obtained experimentally in Table 13. It can be clearly seen that the developed CG model for the copolymer gives an accurate description of the CMC.

Table 13. Critical micelle concentration (mmol/L) for the $MePEG_{17}$-b-PCL_2 system at 310K

Number of free monomers (last 100ns)	**CMC (Simulation)**	**CMC (Experimental- Letchford et al.[43])**
7±2	1.40 ± 0.40	1.89

Chapter 5

Implicit solvent simulations: Transferability and Validation

5.1 Introduction

Implicit solvent simulations have been gaining a lot of popularity of late, due to the straightforward computational speedup that they provide when exploring systems over large spatial and temporal scales. The implicit solvent version of the MARTINI force field, dubbed the "Dry MARTINI" force field (Arnarez et al.[32]) is a systematically parametrized solvent-free version of the "wet MARTINI" force field, developed for the simulations of large and complicated bilayer membranes with millions of lipids.

Extensions of the Dry MARTINI force field to polymers have been explored very recently to study significantly large systems involving polymers. One such model is that developed for Polyethylene oxide (PEO) by Wang and Larson[44], to study the self-assembly and phase behavior of surfactant systems based on PEO. Since PCL based nanoparticles are widely applied in drug delivery systems, extension of the PCL CG potential developed above, to the Dry MARTINI force field is a logical choice that would enable the study of complex systems such as nanoparticle bilayer interactions, which form a crucial step in the endocytosis of these nano-carriers. Therefore, in the forthcoming sections, the extension of the PCL CG potential to the Dry MARTINI framework, and its validation are discussed.

5.2 Transferability to the "Dry" MARTINI forcefield

In order to test the transferability of the developed intramolecular interactions for the PCL homopolymer (bond stretching, angle bending), simulations were performed on both, dilute melts of short PCL chains, as well as isolated long chains of the PCL homopolymer in an implicit solvent setup. The non-bonded interaction parameters were taken from those developed by Arnarez et al.[32] as part of the Dry MARTINI formulation. The bond stretching and angle bending potentials developed above (Chapter 2, Table 1), were used as the initial starting guess in the implicit solvent simulations, and the resulting distributions of distances and angles between the CG beads were matched with the distributions obtained from the explicit solvent MARTINI simulations described previously (Chapter 2, Fig.2). We found that the bond stretching and angle bending potentials developed for the explicit solvent version of the PCL homopolymer are directly transferable to the implicit solvent version as well. The matching distributions obtained between the "dry" and "wet" MARTINI versions are shown in Fig.8.

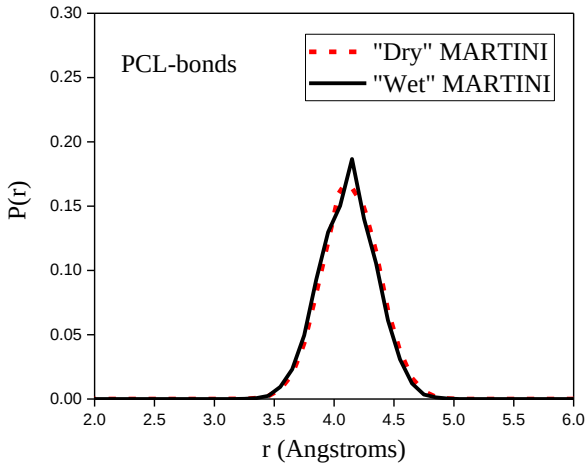

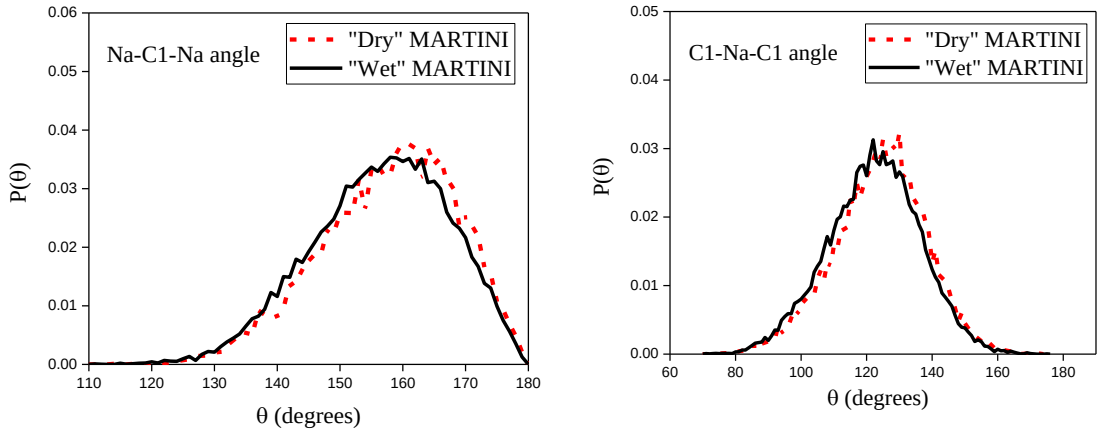

Fig.8 PCL bond and angle distributions between “Dry” and “Wet” MARTINI.

5.3 Conformation of PCL homopolymers: “Dry” vs “Wet” MARTINI

In order to validate the transferability of the developed CG potential to the implicit solvent system, the conformation of select isolated long chain PCL homopolymers at 300K, were simulated in both the implicit and explicit solvent setup. The resulting time averaged radius of gyration and principle moments of the gyration tensor were compared between the “Dry” and “Wet” MARTINI simulations, and are given in Tables 14 and 15 respectively. It can clearly be seen that the implicit solvent simulations give an accurate radius of gyration and predict a similar shape for the homopolymers as those obtained from the explicit solvent simulations. Adding to this, the computational speedup obtained with the implicit solvent simulation makes it a very handy technique for studying the conformational and structural properties of long chain polymers. The validation of the transferred CG potential for the PCL homopolymer to an implicit solvent setup, also

paves the way for studying the interaction of PCL based nanoparticles with realistic membranes composed of millions of lipids, as seen in mammalian cells.

Table 14. Time averaged radius of gyration (nm) of PCL homopolymers (mean ± SD) at 300K ("Dry" vs "Wet" MARTINI)

N	"Wet" MARTINI	"Dry" MARTINI
200	1.673 ± 0.013	1.670 ± 0.012
225	1.741 ± 0.014	1.736 ± 0.010
250	1.804 ± 0.015	1.798 ± 0.011
275	1.855 ± 0.011	1.853 ± 0.010
300	1.911 ± 0.012	1.908 ± 0.010

Table 15. Time averaged principle moments of the gyration tensor (nm) of PCL homopolymers (mean ± SD) at 300K ("Dry" vs "Wet" MARTINI)

N	"Wet" MARTINI			"Dry" MARTINI		
	λ_1	λ_2	λ_3	λ_1	λ_2	λ_3
200	1.07 ± 0.04	0.95 ± 0.03	0.87 ± 0.03	1.05 ± 0.04	0.96 ± 0.03	0.87 ± 0.03
225	1.11 ± 0.04	1.00 ± 0.03	0.90 ± 0.03	1.09 ± 0.04	0.99 ± 0.02	0.92 ± 0.03
250	1.16 ± 0.05	1.04 ± 0.03	0.92 ± 0.04	1.13 ± 0.04	1.03 ± 0.03	0.94 ± 0.03
275	1.18 ± 0.04	1.06 ± 0.03	0.97 ± 0.03	1.16 ± 0.03	1.06 ± 0.02	0.98 ± 0.03
300	1.21 ± 0.04	1.09 ± 0.03	1.00 ± 0.03	1.19 ± 0.04	1.09 ± 0.03	1.01 ± 0.03

Chapter 6

Summary and Conclusion

In this work, we have developed a coarse-grained model for the biocompatible hydrophobic polyester polycaprolactone (PCL) within the framework of the MARTINI-CG force field. Due to its numerous applications in drug delivery as self-assembled micelles formed from block copolymers with polyethylene glycol (MePEG), we also parametrized a model for the linear MePEG-b-PCL diblock copolymer, using an existing model for MePEG. The developed model for the PCL homopolymer was initially validated by analysing its conformational properties such as end to end distance, radius of gyration and principal moments in water at ambient conditions, for polymers of different chain lengths. We found excellent agreement of the structural properties against those predicted from atomistic simulations. We also tested the temperature and solvent transferability of the developed model by analysing structural properties of select PCL homopolymers. The model showed good temperature transferability, and overall a reasonable solvent transferability as well. We note that care must be taken when modelling the conformation of the homopolymers in a typical solvent anti-solvent mixture such as the acetone-water mixture investigated here. Dynamics of the homopolymers in solution were also studied by computing the hydrodynamic radius, which also showed good agreement with the atomistic results.

The developed copolymer model for the MePEG-b-PCL system was validated by studying the self-assembly of the amphiphilic molecules in water. Two separate systems (*$MePEG_{17}$-b-PCL_3* and *$MePEG_{17}$-b-PCL_2*) were investigated. The amphiphiles self-assembled rapidly, initially forming small aggregates which later combined to form large spherical micelles

with a typical core-shell morphology. The hydrophobic PCL constituted the core while the shell was composed of the hydrophilic MePEG. Detailed analysis on the shape showed that the aggregates were nearly spherical, with a very low asphericity. The size of the aggregates was characterized by the hydrodynamic diameter and compared with reported experimental values. In both the systems investigated, we found that the hydrodynamic diameter was under-predicted in comparison to the experimentally measured size of the micelles. The reason behind this is attributed to the finite system size and simulation time which prevents the formation of very large micelles. Also, we computed the critical micelle concentration (CMC) for the $MePEG_{17}$-b-PCL_2 system, which showed quantitative agreement with the experimental CMC. Due to the growing popularity of implicit solvent simulations, the transferability of the developed CG potential to a solvent-free version of the MARTINI force field was analyzed. We found that the CG potential for the PCL homopolymer (bond stretching, angle bending) developed for the explicit solvent version were directly transferable to the implicit solvent "Dry" MARTINI system as well. This was further validated by analyzing the conformation of select long chain PCL homopolymers in an explicit solvent vs implicit solvent setup, which yielded excellent results.

Overall, the developed MARTINI-CG model for PCL proves to be a robust coarse-grained model for this biologically important polymer, paving the way for the development of models for other polymers with applications to bettering human health. Since the model is developed within the framework of a well-established biomolecular force field, we hope that it aids in the study of more complex systems such as the interaction of PCL based nanoparticles with lipids, proteins and other biomolecules.

References

(1) Woodruff, M.A., Hutmacher, D.W., The return of a forgotten polymer-Polycaprolactone in the 21st century. *Progress in Polymer Science* 2010, 35, 1217–1256.

(2) Jabr-Milane, L.S., van Vlerken, L.E., Yadav, S., Amiji, M.M., Multi-functional nanocarriers to overcome tumor drug resistance. *Cancer Treat. Rev*. 2008, 34, 592–602.

(3) Dash, T.K., Konkimalla, V.B., Polymeric Modification and Its Implication in Drug Delivery: Poly-ε-caprolactone (PCL) as a Model Polymer. *Mol. Pharm*. 2012, 9, 2365–2379.

(4) Kataoka, K., Harada, A., Nagasaki, Y., Block copolymer micelles for drug delivery: design, characterization and biological significance. *Adv. Drug Deliv. Rev.* 2001, 47, 113–131.

(5) Adams, M.L., Lavasanifar, A., Kwon, G.S., Amphiphilic block copolymers for drug delivery. *J. Pharm. Sci.* 2003, 92, 1343–1355.

(6) Kao, H.-W., Chan, C.-J., Chang, Y.-C., Hsu, Y.-H., Lu, M., Shian-Jy Wang, J., Lin, Y.-Y., Wang, S.-J., Wang, H.-E., A pharmacokinetics study of radiolabeled micelles of a poly(ethylene glycol)-block-poly(caprolactone) copolymer in a colon carcinoma-bearing mouse model. *Appl. Radiat. Isot.* 2013, 80, 88–94.

(7) Diao, Y.-Y., Li, H.-Y., Fu, Y.-H., Han, M., Hu, Y.-L., Jiang, H.-L., Tsutsumi, Y., Wei, Q.-C., Chen, D.-W., Gao, J.-Q., Doxorubicin-loaded PEG-PCL copolymer micelles enhance cytotoxicity and intracellular accumulation of doxorubicin in adriamycin-resistant tumor cells. *Int. J. Nanomedicine* 2011, 6, 1955–1962.

(8) Huynh, L., Neale, C., Pomès, R., Allen, C., Systematic design of unimolecular star copolymer micelles using molecular dynamics simulations. *Soft Matter* 2010, 6, 5491–5501.

(9) Thota, N., Luo, Z., Hu, Z., Jiang, J., Self-Assembly of Amphiphilic Peptide (AF)6H5K15: Coarse-Grained Molecular Dynamics Simulation. *J. Phys. Chem. B* 2013, 117, 9690–9698.

(10) Nie, S.Y., Sun, Y., Lin, W.J., Wu, W.S., Guo, X.D., Qian, Y., Zhang, L.J., Dissipative Particle Dynamics Studies of Doxorubicin-Loaded Micelles Assembled from Four-Arm Star Triblock Polymers 4AS-PCL-b-PDEAEMA-b-PPEGMA and their pH-Release Mechanism. *J. Phys. Chem. B* 2013, 117, 13688–13697.

(11) Thota, N., Jiang, J., Computational amphiphilic materials for drug delivery. *Front. Mater*. 2015, 2, 64.

(12) Loverde, S.M., Klein, M.L., Discher, D.E., Nanoparticle Shape Improves Delivery: Rational Coarse Grain Molecular Dynamics (rCG-MD) of Taxol in Worm-Like PEG-PCL Micelles. *Adv. Mater.* 2012, 24, 3823–3830.

(13) Marrink, S.J., Risselada, H.J., Yefimov, S., Tieleman, D.P., de Vries, A.H., The MARTINI Force Field: Coarse Grained Model for Biomolecular Simulations. *J. Phys. Chem. B* 2007, 111, 7812–7824.

(14) Marrink, S.J., Tieleman, D.P., Perspective on the Martini model. *Chem. Soc. Rev.* 2013, 42, 6801–6822.

(15) Lee, H., de Vries, A.H., Marrink, S.-J., Pastor, R.W., A Coarse-Grained Model for Polyethylene Oxide and Polyethylene Glycol: Conformation and Hydrodynamics. *J. Phys. Chem. B* 2009, 113, 13186–13194.

(16) Rossi, G., Monticelli, L., Puisto, S.R., Vattulainen, I., Ala-Nissila, T., Coarse-graining polymers with the MARTINI force-field: polystyrene as a benchmark case. *Soft Matter* 2011, 7, 698–708.

(17) Lee, H., Larson, R.G., Molecular Dynamics Simulations of PAMAM Dendrimer-Induced Pore Formation in DPPC Bilayers with a Coarse-Grained Model. *J. Phys. Chem. B* 2006, 110, 18204–18211.

(18) Nawaz, S., Carbone, P., Coarse-Graining Poly(ethylene oxide)–Poly(propylene oxide)–Poly(ethylene oxide) (PEO–PPO–PEO) Block Copolymers Using the MARTINI Force Field. *J. Phys. Chem. B* 2014, 118, 1648–1659.

(19) Lee, H., Larson, R.G., Molecular Dynamics Study of the Structure and Interparticle Interactions of Polyethylene Glycol-Conjugated PAMAM Dendrimers. *J. Phys. Chem. B* 2009, 113, 13202–13207

(20) Lee, H., Pastor, R.W., Coarse-Grained Model for PEGylated Lipids: Effect of PEGylation on the Size and Shape of Self-Assembled Structures. *J. Phys. Chem. B* 2011, 115, 7830–7837.

(21) Jorgensen, W.L., Madura, J.D., Swenson, C.J., Optimized intermolecular potential functions for liquid hydrocarbons. *J. Am. Chem. Soc.* 1984, 106, 6638–6646.

(22) Jorgensen, W.L., Maxwell, D.S., Tirado-Rives, J., Development and Testing of the OPLS All-Atom Force Field on Conformational Energetics and Properties of Organic Liquids. *J. Am. Chem. Soc.* 1996, 118, 11225–11236.

(23) Berendsen, H. J. C.; Postma, J. P. M.; van Gusteren, W. F.; Hermans, *J. Intermolecular Forces*; Reidel: Dordrecht, 1981.

(24) Pronk, S., Páll, S., Schulz, R., Larsson, P., Bjelkmar, P., Apostolov, R., Shirts, M.R., Smith, J.C., Kasson, P.M., Spoel, D. van der, Hess, B., Lindahl, E., GROMACS 4.5: a high-throughput and highly parallel open source molecular simulation toolkit. *Bioinformatics* 2013, 29, 845–854.

(25) Abraham, M.J., Murtola, T., Schulz, R., Páll, S., Smith, J.C., Hess, B., Lindahl, E., GROMACS: High performance molecular simulations through multi-level parallelism from laptops to supercomputers. *SoftwareX* 2015, 1–2, 19–25.

(26) Hess, B., Bekker, H., Berendsen, H.J.C., Fraaije, J.G.E.M., LINCS: A linear constraint solver for molecular simulations. *J. Comput. Chem.* 1997, 18, 1463–1472.

(27) Darden, T., York, D., Pedersen, L., Particle mesh Ewald: An N·log(N) method for Ewald sums in large systems. *J. Chem. Phys.* 1993, 98, 10089–10092.

(28) Bussi, G., Donadio, D., Parrinello, M., Canonical sampling through velocity rescaling. *J. Chem. Phys.* 2007, 126, 014101.

(29) Berendsen, H.J.C., Postma, J.P.M., Gunsteren, W.F. van, DiNola, A., Haak, J.R., Molecular dynamics with coupling to an external bath. *J. Chem. Phys.* 1984, 81, 3684–3690.

(30) Parrinello, M., Rahman, A., Polymorphic transitions in single crystals: A new molecular dynamics method. *J. Appl. Phys.* 1981, 52, 7182–7190.

(31) Bulacu, M., Goga, N., Zhao, W., Rossi, G., Monticelli, L., Periole, X., Tieleman, D.P., Marrink, S.J., Improved Angle Potentials for Coarse-Grained Molecular Dynamics Simulations. *J. Chem. Theory Comput.* 2013, 9, 3282–3292.

(32) Arnarez, C., Uusitalo, J.J., Masman, M.F., et al., Dry Martini, a coarse-grained force field for lipid membrane simulations with implicit solvent, *J. Chem. Theory Comput.* 2015, 11, 260-275.

(33) Di Pasquale, N., Marchisio, D.L., Barresi, A.A., Carbone, P., Solvent Structuring and Its Effect on the Polymer Structure and Processability: The Case of Water–Acetone Poly-ε-caprolactone Mixtures. *J. Phys. Chem. B* 2014, 118, 13258–13267.

(34) Rubinstein, M.; Colby, R. H. *Polymer Physics*; Oxford University Press: New York, 2003.

(35) Carbone, P., Varzaneh, H.A.K., Chen, X., Müller-Plathe, F., Transferability of coarse-grained force fields: the polymer case. *J. Chem. Phys.* 2008, 128, 064904.

(36) Fuhrmans, M., Sanders, B.P., Marrink, S.-J., Vries, A.H. de, Effects of bundling on the properties of the SPC water model. *Theor. Chem. Acc.* 2009, 125, 335–344.

(37) Hess, B., Determining the shear viscosity of model liquids from molecular dynamics simulations. *J. Chem. Phys.* 2002, 116, 209–217.

(38) Yeh, I.-C., Hummer, G., System-Size Dependence of Diffusion Coefficients and Viscosities from Molecular Dynamics Simulations with Periodic Boundary Conditions. *J. Phys. Chem. B* 2004, 108, 15873–15879.

(39) Lince, F., Marchisio, D.L., Barresi, A.A., Strategies to control the particle size distribution of poly-ε-caprolactone nanoparticles for pharmaceutical applications. *J. Colloid Interface Sci.* 2008, 322, 505–515.

(40) Zelenková, T., Fissore, D., Marchisio, D.L., Barresi, A.A., Size control in production and freeze-drying of poly-ε-caprolactone nanoparticles. *J. Pharm. Sci.* 2014, 103, 1839–1850.

(41) Yesylevskyy, S.O., Schäfer, L.V., Sengupta, D., Marrink, S.J., Polarizable Water Model for the Coarse-Grained MARTINI Force Field. *PLoS Comput Biol* 2010, 6, e1000810

(42) Cheng, Jianli, Vishnyakov, A., Neimark, A.V., Morphological Transformations in Polymer Brushes in Binary Mixtures: DPD Study. *Langmuir* 2014, 30, 12932–12940.

(43) Letchford, K., Liggins, R., Burt, H., Solubilization of hydrophobic drugs by methoxy poly(ethylene glycol)-block-polycaprolactone diblock copolymer micelles: Theoretical and experimental data and correlations. *J. Pharm. Sci.* 2008, 97, 1179–1190.

(44) Wang, S., Larson, R.G., A coarse-grained implicit solvent model for poly(ethylene oxide), CnEm surfactants, and hydrophobically end-capped poly(ethylene oxide) and its application to micelle self-assembly and phase behavior. *Macromolecules* 2015, 48, 7709-7718.